Preliminary Assessment for Space-Debris Reentry as an Initiating Event in PSA

Haeun Jo, Gyunyoung Heo*
Department of Nuclear Engineering, College of Engineering, Kyung Hee University, Yongin, Republic of Korea
**Corresponding Author: gheo@khu.ac.kr*

***Keywords : Space debris reentry, Nuclear power plant, Probabilistic Safety Assessment, External Hazards**

1. Introduction

The space sector is undergoing a rapid transition from a government-led exploration paradigm to a private-sector-driven New Space era. In particular, mega-constellation programs—such as SpaceX's *Starlink* and Amazon's *Project Kuiper*—are being deployed worldwide to establish highly connected low Earth Orbit (LEO) communications networks. Recent assessments by the European Space Agency (ESA) indicate that, as of 2025, the number of trackable objects in orbit has exceeded approximately 40,000, while the population of small fragments larger than 1 cm—beyond the effective resolution of current tracking systems—is estimated to be on the order of one million or more.

As illustrated in Fig. 1, the historical trend of objects in Earth orbit demonstrates a stark contrast between LEO and other orbital regimes (MEO, GEO, and super-GEO). While the object populations in higher orbits have grown gradually, the LEO environment has experienced unprecedented, nearly exponential growth since approximately 2020, directly reflecting the aggressive deployment of commercial mega-constellations. This exponential growth in anthropogenic space objects not only elevates the risk of on-orbit collisions but also results in a substantial increase in the frequency of atmospheric reentries of end-of-life spacecraft.

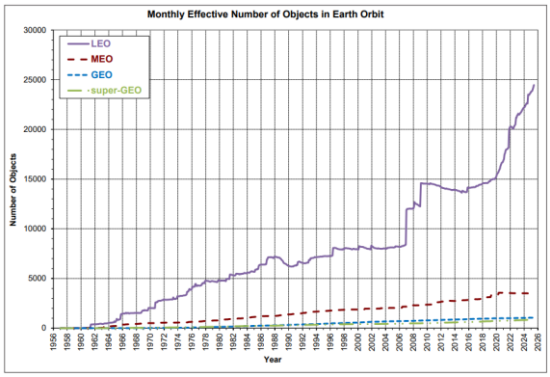

Fig 1. Monthly Effective Number of Objects in Earth Orbit [1]

In general, objects reentering the atmosphere are expected to largely ablate due to severe aerodynamic heating. However, with the trend toward larger spacecraft and the increasing use of high-temperature structural materials (e.g., titanium, stainless steel, and carbon composites), the quantity of surviving fragments reaching the ground can no longer be regarded as negligible. Reentry survivability and ground-risk evaluations conducted by organizations such as NASA's Orbital Debris Program Office suggest that a nontrivial fraction of an object's mass may survive reentry, implying that hundreds of tons of artificial debris can reach the surface at unpredictable locations each year. In particular, for uncontrolled reentries, the impact location is difficult to predict with practical accuracy in advance; therefore, such events may pose a tangible physical threat to critical national infrastructure.

Nuclear power plants (NPPs) are essential assets for national energy security and are required to maintain exceptionally high levels of protection against external hazards. Their safety is managed quantitatively through probabilistic safety assessment (PSA). In the context of external, human-induced hazards such as aircraft crashes or explosions, the IAEA Safety Guide SSG-79 discusses the use of a screening probability level (SPL) to determine whether a given hazard warrants detailed evaluation; a screening level on the order of $1.0 \times 10^{-7} yr^{-1}$ is commonly used as a conservative criterion in this context. However, existing PSA models have not yet sufficiently incorporated engineering evaluations of space-debris ground-impact hazards in a manner that reflects the rapidly evolving space environment.

In the Republic of Korea, operating NPP sites are concentrated within a limited latitude band. Given the orbital inclination characteristics of space objects, mid-latitude regions fall within latitude ranges associated with relatively elevated ground-impact likelihood. If space debris strikes vulnerable portions of an NPP, the resulting hypervelocity impact could be treated as a candidate initiating event. Accordingly, this paper recalculates the ground-impact probability of space debris using updated data reflecting current launch and deployment trends in the New Space era and performs a preliminary assessment of whether the estimated frequency exceeds the initiating-event screening cutoff.

2. Recent Trends in Space Debris and Future Outlook

2.1. The New Space Paradigm and Orbital Congestion

Unlike earlier eras of space development that were largely confined to government-led exploration or strategic objectives, the contemporary New Space era has rapidly shifted toward a paradigm driven by private-sector commercial goals. In particular, competition to secure market leadership in LEO satellite

communications - through mega-constellation programs such as SpaceX's Starlink and Amazon's Project Kuiper - has resulted in an unprecedented surge in orbital congestion.

As of 2026, the number of catalogued objects regularly tracked by space surveillance networks is on the order of 4.5×10^4 [2]. This rapid increase exceeds the cumulative growth of space objects over multiple decades within only a few years. Such growth not only aggravates collision risk, including concerns associated with the Kessler syndrome, but also directly drives an increase in the frequency of atmospheric reentries of end-of-life satellites.

2.2. Physical Survivability Mechanisms of Reentering Objects and Associated Hazards

In general, reentering objects are intended to largely demise due to intense aerothermal heating during high-velocity atmospheric entry. In practice, however, it is increasingly common for specific spacecraft components to survive reentry and reach the ground. Components such as propellant tanks, attitude-control reaction wheels, and major engine hardware are often manufactured from high-melting-point materials (e.g., titanium alloys and stainless steels) to ensure mechanical robustness and extreme thermal resistance. Consequently, such components may retain their physical integrity and reach the surface even under severe thermal loads on the order of 1,500 °C during reentry. Published reentry survivability studies commonly indicate that, depending on object design and materials, roughly 10% to 40% of the pre-reentry mass of large objects may survive as ground-reaching fragments.

These fragments can accelerate to terminal velocity in free fall and, while retaining substantial mass, may act as potential impactors capable of delivering significant kinetic energy to NPP structures, including the containment building and safety-related equipment. From an external-hazards perspective, ground impacts by surviving fragments therefore warrant consideration as a credible physical threat mechanism, especially for vulnerable plant areas.

If the currently planned global satellite-network deployments mature within the next decade, the short replacement cycles typical of such constellations imply that thousands of satellites could reenter the atmosphere annually. Even under scenarios that maintain the present launch cadence, hundreds of reentry events per year may occur, depending on the object categories considered. Furthermore, mid-latitude regions—including the Korean Peninsula—are repeatedly traversed by the orbital-inclination ground tracks of many LEO satellites, implying geographic vulnerability with potentially elevated exposure to ground-impact events relative to the global average. Collectively, these environmental changes suggest that space-debris reentry—previously regarded as negligible—may need to be incorporated into the probabilistic external-hazard spectrum at a level comparable to other projectile-type hazards (e.g., tornado-generated missiles) that are already managed within nuclear power plant design-basis and safety assessment frameworks.

3. Methodology For Assessing Space-debris Impact Risk

A screening-level estimate of ground-impact frequency can be obtained by scaling the global reentry rate by an areal ratio. However, this approach implicitly assumes an isotropic (uniform-area) ground-impact distribution and therefore neglects a key orbital-dynamics constraint: each abandoned rocket body (and many satellites) remains confined to a specific orbital inclination. Because orbital inclination restricts the accessible impact latitudes and results in nonuniform residence time along the ground track, the probability that an uncontrolled object reenters at a given latitude is not spatially uniform and should instead be represented by a latitude-weighting function. As demonstrated in Fig. 2, the spatial distribution of reentry probability is strongly dependent on latitude. The weighting functions for rocket bodies exhibit distinct peaks corresponding to heavily utilized orbital inclinations, in stark contrast to an isotropic distribution. Notably, elevated probabilities appear in specific mid-latitude bands, which are directly relevant to the geographic location of the Korean Peninsula. Accordingly, this study incorporates a latitude-dependent weighting model to allocate global reentry events to the latitude band containing Korean NPP sites and subsequently localizes the allocated events to the effective plant target area using a PSA-consistent two-step framework.

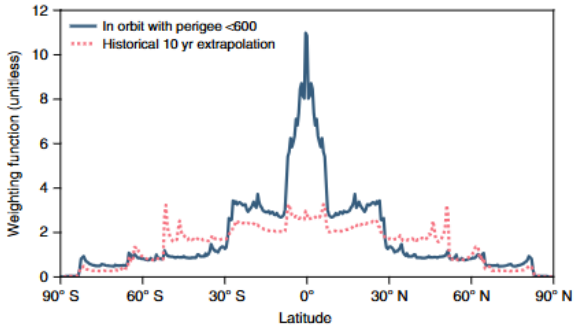

Fig 2. Latitude-dependent rocket-body weighting functions. [3]

3.1. Latitude-dependent allocation model [4]

Objects originating from inclined orbits are bounded in impact latitude by $|\phi| \leq i$. Near the turning latitudes (approximately $\phi \approx \pm i$), the meridional (north–south) component of the ground-track velocity approaches zero, which maximizes dwell time and increases the relative exposure of those latitude regions. This produces a latitude-dependent focusing effect that deviates from isotropy. To represent this effect analytically, we adopt a latitude probability density function (PDF) $\rho(\phi; i)$ such that $\rho(\phi; i)d\phi$ is the probability that an impact occurs

within $[\phi, \phi + d\phi]$, given inclination i. Using the classical orbital-geometry relation for circular orbits, $sin\,\phi = sin\,i\,sin\,u$ (e.g., Kaula, 1966), and assuming a uniform distribution of the argument of latitude uuu, the resulting latitude probability density function is given by:

$$\boldsymbol{\rho(\phi; i) = \frac{\cos\phi}{\pi\sqrt{\sin^2 i - \sin^2\phi}}, |\phi| \le i} \quad (1)$$

And $\rho(\phi; i) = 0$ for $|\phi| > i$. By construction, $\rho(\phi; i)$ satisfies the normalization condition $\int_{-i}^{i} \rho(\phi; i) d\phi = 1$.

Let $[\phi_1, \phi_2]$ denote the latitude band that contains domestic NPP sites (here, 34°N–38°N). The probability that an impact occurs within this latitude band is: (

$$\boldsymbol{P_{band} = \int_{\phi_1}^{\phi_2} \rho(\phi; i)\, d\phi} \quad (2)$$

To separate orbital-mechanics-driven concentration from trivial geometric area effects, we compute the geometric surface-area ratio of the same latitude band. The surface area of a spherical zone between $\phi_1 and\ \phi_2$is:

$$\boldsymbol{A_{lat\_band} = 2\pi R^2(\sin\phi_2 - \sin\phi_1)} \quad (3)$$

where R is the mean Earth radius. The corresponding dimensionless area ratio relative to the Earth's surface area $A_{earth} = 4\pi R^2$ is:

$$\boldsymbol{Area_{ratio} = \frac{A_{lat\_band}}{A_{earth}} = \frac{\sin\phi_2 - \sin\phi_1}{2}} \quad (4)$$

Using (2) and (4), we define a latitude bias (or latitude weighting) factor:

$$\boldsymbol{F_{lat} = \frac{P_{band}}{Area_{ratio}}} \quad (5)$$

Here, $F_{lat} > 1$ indicates that impacts are concentrated in the latitude band more than would be expected under an isotropic (uniform-area) distribution. In this study, F_{lat} serves as an interpretable vulnerability indicator, whereas the impact-frequency calculation is based explicitly on the band probabilityP_{band} (Section 3.3).

3.2. Annual impact-frequency model

We model the annual frequency of NPP-relevant debris impacts as the product of (i) the global re-entry event rate, (ii) the conditional probability that a re-entry produces ground-reaching fragments, (iii) the conditional probability that those fragments capable of producing meaningful structural damage, (iv) the probability of allocation to the latitude band of interest, and (v) the areal fraction that localizes impacts to the effective plant target area within that band. The resulting annual impact frequency is:

$$\boldsymbol{P_{annual} = \lambda_{global} \times P_{survive} \times P_{dmg} \times P_{band} \times \frac{A_{target}}{A_{band}}} \quad (6)$$

This formulation reflects a PSA-consistent two-step localization. Global re-entry events are first allocated to the latitude band with probability P_{band}(Stage 1), and then localized to the plant target within that band by the areal fraction A_{target}/A_{lat_band} (Stage 2). The output P_{annual} is expressed in units of yr^{-1}, enabling direct comparison with initiating-event screening criteria.

3.3. Definition of variables and implementation details

1) $\boldsymbol{\lambda_{global}}$(global annual re-entry event rate,yr^{-1}).

$\boldsymbol{\lambda_{global}}$ denotes the expected annual number of re-entry events considered in the screening model. It is set with reference to publicly available orbital-environment statistics reported by organizations such as NASA and ESA. A baseline value of 1,350 events per year is used for the reference year (2026), and a scenario with increased re-entry activity is considered for 2036–2056 to reflect accelerated end-of-life disposal and replacement cycles associated with mega-constellations. For screening purposes, $\boldsymbol{\lambda_{global}}$ is treated as a Poisson event rate.

2) $P_{survive}$ (ground-reaching fragment survivability probability, dimensionless).

$P_{survive}$ is the conditional probability that a re-entering object does not fully demise due to aerothermal heating and produces at least one ground-reaching fragment of non-negligible mass. This study adopts a conservative screening value of $P_{survive} = 0.25$, intended to represent an average survivability level consistent with common re-entry survivability considerations for large objects and high-temperature materials. The parameter is treated as a single screening-level input rather than an object-specific breakup/survivability simulation.

3) P_{dmg} (damage effectiveness factor, dimensionless).

P_{dmg} While most surviving fragments are relatively small and possess limited impact energy, certain high-mass components—such as titanium propellant tanks or major engine hardware—may retain sufficient kinetic energy at terminal velocity to challenge structural resistance. In the absence of impact-fragility data for NPP structures subjected to such debris, this study adopts $P_{dmg} = 0.1$ as a conservative screening assumption to represent the energetically significant subset of the debris population, rather than as an empirically derived statistical constant.

4) i (representative orbital inclination, degrees).

i denotes the representative inclination of the dominant LEO constellation population used in the model. A baseline value of $i = 53^{\circ}$ is used to compute the latitude distribution via (1) and the latitude-band probability P_{band} via (2) If multiple inclinations contribute significantly, the model can be extended by using an inclination mixture $\rho(\phi) = \sum_k w_k\, \rho(\phi; i_k)$; but a single representative inclination is adopted here for a preliminary screening assessment.

5) ϕ, ϕ_1, ϕ_2 (latitude variables, degrees).

ϕ is geographic latitude. $[\phi_1, \phi_2]$ defines the latitude band of interest for domestic NPP sites. This study uses $\phi_1 = 34^{\circ}N$ and $\phi_2 = 38^{\circ}N$.

6) F_{lat} (latitude bias factor, dimensionless).
F_{lat} is a concentration metric defined by (5). It measures how strongly impacts are concentrated within the latitude band relative to isotropic expectation. For the representative inclination $i = 53^{\circ}$, a value of $F_{lat} = 1.25$ is applied to describe the geographic exposure tendency; the impact-frequency calculation itself uses P_{band} explicitly in (6) to preserve the two-step localization interpretation.

7) A_{target}(effective target area, km^2)
A_{target} is the effective "threat-relevant" target footprint representing plant areas where major structures sensitive to external impacts are concentrated. For each unit, a conservative rectangular footprint of 215 m by 105 m is adopted, corresponding to $0.0226km^2$. Applying this footprint uniformly to 26 domestic units (operating and under construction) yields a total effective target area of: $A_{target} = 26 \times 0.0226 \approx 0.588$

8) A_{band} (latitude-band surface area, km^2).
A_{band} denotes the Earth's surface area within 34°N–38°N. Assuming a spherical Earth with mean radius $R = 6{,}371km$, substituting $\phi_1 = 34^{\circ}N$ and $\phi_2 = 38^{\circ}N$ into (3) yields: $A_{lat\_band} \approx 1.44 \times 10^7 km^2$). This corresponds to approximately 2.82% of the Earth's total surface area($\approx 5.1 \times 10^8 km^2$). In (6), A_{band} serves as the normalization denominator for within-band areal localization, converting a latitude-band allocation into an expected site-impact frequency.

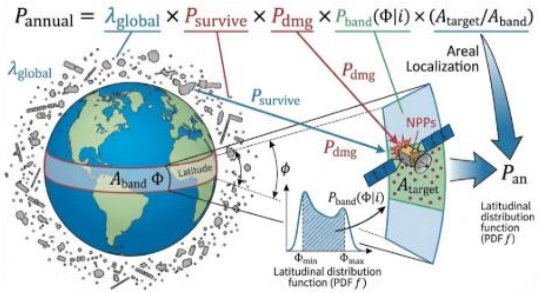

Fig 3. Annual Impact Probability Model

4. Data Analysis and Results

4.1 Derivation of the Effective Target Area (A_{target}) and Conservative Screening Basis

To enhance the credibility of the debris-impact frequency estimation, this study departs from the conventional approach of summing only the plan areas of selected safety-classified buildings and instead introduces a **site-based effective target area** concept. Within a nuclear power plant (NPP) site, safety-significant systems are spatially distributed, including not only the containment structure but also emergency diesel generators (EDGs), intake structures, switchyard equipment, and other balance-of-plant systems essential for safe shutdown. A debris impact affecting any of these structures may initiate complex multi-system challenges and thus constitutes a potential PSA-relevant initiating event.

Using high-resolution satellite imagery obtained from Google Earth (accessed March 2026), the core operational region of the Hanbit NPP site—adopted as a representative domestic reference model—was delineated and measured. The area encompassing the containment building and major auxiliary safety-related structures was conservatively approximated as a rectangular region with dimensions of approximately 0.215 km (width) and 0.105 km (length), corresponding to an area of 0.0226 km² per unit.

Extending this footprint to all 26 operating and under-construction units nationwide yields a total effective target area: $A_{target} = 0.588\text{km}^2$. This value exceeds the plan area of containment domes alone but excludes nonessential green areas and peripheral zones. Therefore, it represents a conservative approximation of the effective threat region capable of generating an initiating challenge to plant safety functions.

Fig 4. Effective Target Area of Hanbit NPP

4.2 Global Annual Reentry Rate Based on ESA Statistics

According to the ESA Space Environment Report 2025, intact satellites or rocket bodies are currently reentering the atmosphere at an average rate exceeding three per day. When converted to an annual basis, this corresponds to more than 1,100 reentries per year. Furthermore, the ESA Space Debris User Portal (MASTER-8 reference population) indicates that the number of tracked orbital objects larger than 10 cm has reached approximately 54,000. By normalizing the observed annual reentry count to the total tracked population, an effective annual decay fraction of approximately 2.1% can be derived. However, the period 2025–2026 corresponds to the peak phase of Solar Cycle 25, during which enhanced upper-atmospheric density increases aerodynamic drag in LEO,

thereby shortening orbital lifetimes and accelerating reentry rates. In addition, recent policy shifts—such as the adoption of a 5-year post-mission disposal guideline—are expected to increase intentional deorbiting activities.

Considering these environmental and regulatory drivers, this study adopts a conservative screening decay fraction of 2.5% for 2026. Accordingly, the global annual reentry rate is defined as: $\lambda_{global} = 1350 yr^{-1}$.

To reflect the expansion of mega-constellations and the increasing orbital object population in the New Space environment, future reentry rates are defined using a scenario-based projection. Assuming the same conservative decay fraction (2.5%) and growth in the tracked object population, the following values are adopted: $\lambda_{global}(2036) = 2{,}760 yr^{-1}$, $\lambda_{global}(2056) = 4{,}625 yr^{-1}$. These values represent screening-level projections consistent with anticipated constellation deployment and replenishment cycles.

4.3 Annual Impact Frequency and Screening Comparison

Using the annual collision frequency formulation defined in Section 3, and adopting $P_{survive} = 0.25$ and $P_{dmg} = 0.1$, the annual impact frequency was calculated for each scenario.

1) 2026 Scenario ($\lambda_{global} = 1{,}350 yr^{-1}$)

The resulting annual impact frequency is: $P_{2026} = 4.59 \times 10^{-8}/yr$. This value remains below the commonly referenced regulatory screening threshold of $10^{-7} yr^{-1}$. From a PSA perspective, this indicates that under current orbital population conditions and structural protection characteristics of domestic containment systems, space-debris impact risk remains screened out as a negligible initiating event. Existing safety management frameworks therefore provide sufficient margin under present conditions.

2) 2036 Scenario ($\lambda_{global}(2036) = 2{,}760 yr^{-1}$)

The calculated annual impact frequency is: $P_{2036} = 9.38 \times 10^{-8}/yr$. This value remains below the commonly referenced regulatory screening threshold of $10^{-7} yr^{-1}$, although the margin is significantly reduced compared to the present baseline scenario. From a PSA perspective, the 2036 projection indicates that space-debris impact remains a screened-out external hazard under the assumed decay-rate scenario; however, the decreasing safety margin suggests that the hazard is approaching the screening boundary.

Accordingly, while immediate design modification or deterministic mitigation measures may not yet be warranted, enhanced monitoring of global reentry trends and periodic reassessment of λ_{global} would be prudent within the external event PSA update cycle. In particular, uncertainties associated with constellation growth, disposal compliance, and solar-activity-driven atmospheric drag could materially influence the projected frequency in the mid-term horizon.

3) 2056 Scenario ($\lambda_{global}(2056) = 4{,}625 yr^{-1}$)

The calculated annual impact frequency is: $P_{2056} = 1.57 \times 10^{-7}/yr$. From a nuclear safety management perspective, an initiating frequency of this magnitude is comparable to certain traditional external hazards considered. Given that the 2056 horizon overlaps with extended operation of existing units and the design life of new reactors, proactive design reinforcement—such as enhanced roof shielding or impact energy dissipation structures—may warrant evaluation during life-extension or new-build licensing reviews.

5. Conclusion

This study conducted a preliminary PSA-based screening of space-debris reentry impacts on nuclear power plants under the evolving New Space environment. To address the limitations of isotropic area-scaling approaches, a latitude-weighted allocation model reflecting orbital inclination characteristics was developed, enabling inclination-informed localization of global reentry events. In addition, a site-based effective target area concept was introduced to conservatively represent safety-significant plant structures relevant to initiating-event screening. The analysis demonstrates that, while current reentry conditions remain generally below the commonly referenced external-hazard screening threshold, projected long-term growth in orbital populations may challenge this margin. These findings confirm that space-debris reentry, though historically neglected in nuclear safety assessments, warrants structured consideration within the external-event PSA framework as orbital activity continues to expand. Overall, this study establishes a methodological foundation for incorporating inclination-informed debris-impact assessment into future PSA evaluations and regulatory screening processes.

Acknowledgement

This work was supported by the Nuclear Safety Research Program through the Regulatory Research Management Agency for SMRS (RMAS) and the Nuclear Safety and Security Commission (NSSC) of the Republic of Korea (No. 1500-1501-409).

REFERENCES

[1] National Aeronautics and Space Administration (NASA), "Orbital Debris Quarterly News," Vol. 29, No. 3, p. 9, Sept. 2025.

[2] European Space Agency (ESA), "Space debris by the numbers," [Online]. Available: https://www.esa.int/Space_Safety/Space_Debris/Space_debris_by_the_numbers (accessed Oct. 24, 2025).

[3] M. Byers, D. Wright, A. MacLean, and A. C. Boley, "Unnecessary risks created by uncontrolled rocket reentries," *Nature Astronomy*, vol. 6, no. 10, pp. 1093–1097, Oct. 2022.

[4] W. M. Kaula, *Theory of Satellite Geodesy*. Waltham, MA: Blaisdell, 1966.